

Divergent Substrate-Binding Mechanisms Reveal an Evolutionary Specialization of Eukaryotic Prefoldin Compared to Its Archaeal Counterpart

Jaime Martín-Benito,¹ Juan Gómez-Reino,¹ Peter C. Stirling,² Victor F. Lundin,² Paulino Gómez-Puertas,³ Jasminka Boskovic,^{1,6} Pablo Chacón,⁴ José J. Fernández,⁵ José Berenguer,³ Michel R. Leroux,² and José M. Valpuesta^{1,*}

¹ Centro Nacional de Biotecnología, Consejo Superior de Investigaciones Científicas, Campus de la Universidad Autónoma de Madrid, Darwin, 3, 28049 Madrid, Spain

² Department of Molecular Biology and Biochemistry, Simon Fraser University, 8888 University Drive, Burnaby, B.C. Canada V5A 1S6

³ Centro de Biología Molecular Severo Ochoa, CSIC-UAM, Campus de la Universidad Autónoma de Madrid, 28049 Madrid, Spain

⁴ Centro de Investigaciones Biológicas, C.S.I.C., Ramiro de Maeztu 9, 28040 Madrid, Spain

⁵ Departamento de Arquitectura de Computadores y Electrónica, Universidad de Almería, 04120 Almería, Spain

⁶ Present address: Centro Nacional de Investigaciones Oncológicas, Melchor Fernández Almagro, 3, 28029 Madrid, Spain.

*Correspondence: jmv@cnb.uam.es

DOI 10.1016/j.str.2006.11.006

SUMMARY

Prefoldin (PFD) is a molecular chaperone that stabilizes and then delivers unfolded proteins to a chaperonin for facilitated folding. The PFD hexamer has undergone an evolutionary change in subunit composition, from two PFD α and four PFD β subunits in archaea to six different subunits (two α -like and four β -like subunits) in eukaryotes. Here, we show by electron microscopy that PFD from the archaeum *Pyrococcus horikoshii* (PhPFD) selectively uses an increasing number of subunits to interact with nonnative protein substrates of larger sizes. PhPFD stabilizes unfolded proteins by interacting with the distal regions of the chaperone tentacles, a mechanism different from that of eukaryotic PFD, which encapsulates its substrate inside the cavity. This suggests that although the fundamental functions of archaeal and eukaryal PFD are conserved, their mechanism of substrate interaction have diverged, potentially reflecting a narrower range of substrates stabilized by the eukaryotic PFD.

INTRODUCTION

To attain their final conformations, some nonnative proteins need the assistance of a group of proteins termed molecular chaperones (Bukau and Horwich, 1998). These proteins work by preventing the aggregation of a denatured protein or by providing an appropriate environment whereby a nonnative polypeptide can reach the native state by using the information encoded in its own amino acid sequence. It is increasingly evident that a host of chaperones work coordinately in protein-folding path-

ways (Mogk et al., 2001), and one of these protein-folding networks is formed by the eukaryal and archaeal chaperonins and the corresponding prefoldins (PFDs).

Chaperonins consist of 60 kDa proteins assembled into a double-ring, toroidal structure with a cavity where folding takes place. Members of the chaperonin family are divided in two groups, namely those found in eubacteria and in endosymbiotic organelles (group I) (Ellis and Hartl, 1999), or those in the cytosols of archaea and eukarya (group II) (Gutsche et al., 1999; Valpuesta et al., 2005). Archaeal chaperonins ("thermosomes") contain one to three different subunits per ring, whereas the eukaryotic cytosolic chaperonin, termed chaperonin containing TCP-1 (CCT) or TCP-1 Ring Complex (TriC), is assembled from eight different but related subunits (Valpuesta et al., 2005).

Prefoldin (PFD) (Vainberg et al., 1998), alternatively termed Gim Complex (GimC) (Geissler et al., 1998), is a heterohexameric protein composed of two or six different subunits that is exclusively found in archaea and eukaryotes (Vainberg et al., 1998; Geissler et al., 1998; Leroux et al., 1999). Biochemical studies have shown that PFDs bind and stabilize unfolded target polypeptides and subsequently delivers them to chaperonins for completion of folding (Vainberg et al., 1998; Siegers et al., 1999; Hansen et al., 1999). The transfer of substrates from PFD to CCT involves a direct interaction between the two chaperones, as visualized by electron microscopy studies of the eukaryotic chaperones (Martín-Benito et al., 2002). A potentially intriguing difference between the archaeal and eukaryal PFD is that the former may be involved in stabilizing a wide array of proteins in vivo, whereas the latter appears to be restricted to only a few proteins, the principle ones being actin and tubulin (Vainberg et al., 1998; Siegers et al., 1999, 2003; Hansen et al., 1999). The structure of the archaeal PFD from *Methanobacterium thermoautotrophicum* (MtPFD), determined at atomic resolution (Siegert et al., 2000), resembles a jellyfish with a base composed of a double β barrel and six protruding

coiled-coil “tentacles.” Each tentacle belongs to one of the six PhPFD subunits, arranged as two PhPFD α subunits located in the center of the structure and four of the homologous PhPFD β placed at the periphery. This structure is conserved for all PFDs since the three-dimensional reconstruction at 25 Å of human PFD obtained by electron microscopy reveals a structure essentially identical to that of its archaeal counterpart (Martín-Benito et al., 2002).

A central question regarding the substrate-binding mechanism of PFD and its cooperation with a chaperonin to facilitate protein biogenesis is whether the eukaryotic PFD-chaperonin system functions in the same manner as the “simpler” archaeal chaperone system or whether its mode of action has diverged during evolution to acquire specialized functions. In this study, we demonstrate that archaeal PFD interacts with its cognate chaperonin in a manner similar to that of eukaryotic PFD-CCT system, suggesting that the overall cooperative mechanism between the archaeal and eukaryotic chaperones is conserved. However, unlike eukaryotic PFD, which interacts with actin by encapsulating it within its cavity, archaeal PFD binds different substrates near the tips of the tentacles by using a variable number of binding sites to stabilize nonnative proteins of different sizes and shapes. Our results show how archaeal PFD may be well adapted to interacting with many different substrates, reflecting its broad role as chaperone *in vivo*, and consequently suggest that eukaryotic PFD has, at least for actin, evolved a specialized binding surface within its cavity.

RESULTS

Three-Dimensional Structure of PhPFD

The *Pyrococcus horikoshii* PFD oligomer (PhPFD), a small complex of ~87 kDa MW, was purified after coexpression in *E. coli* of its two constituting subunits (PhPFD α and PhPFD β). When observed by electron microscope (EM), and as reported for eukaryotic PFD (Martín-Benito et al., 2002), three orthogonal views were found to be the most frequent (Figure 1A). A three-dimensional reconstruction of PhPFD was generated with 3780 negatively stained particles (Figure 1B). The volume obtained, a base plate from which six arms or coiled coils protrude and form a rectangular cavity, is similar to the atomic structure obtained for the MtPFD homolog (Siegert et al., 2000), but with the PhPFD β subunits closer to the neighboring PhPFD α subunit, as revealed by the docking of the MtPFD atomic structure into the EM map by a flexible docking algorithm (Wriggers et al., 2004) (Figure 1B). This apparent conformational flexibility could be related with the PhPFD ability to interact with a wide range of substrates, as discussed below. The three-dimensional reconstruction of PhPFD is also similar to that of the EM-derived human PFD structure (Martín-Benito et al., 2002). In all cases, the structures generated are consistent with the known function of PFD, namely the transport and protection of unfolded substrate until its delivery into the cytosolic chaperonin cavity (Siegert et al., 2000; Martín-Benito et al., 2002; Lundin et al., 2004).

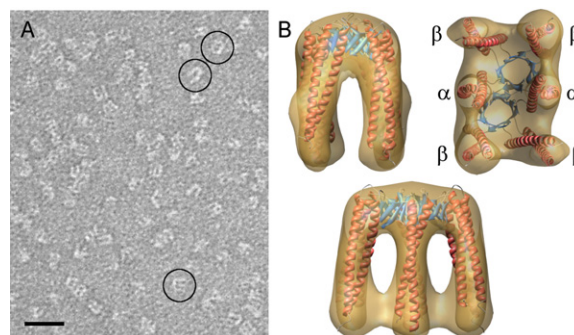


Figure 1. Three-Dimensional Reconstruction of PhPFD

(A) Electron micrograph showing an average field of negatively stained PhPFD particles. The three orthogonal views corresponding to the most common projections presented in the micrograph are encircled. Bar represents 250 Å.

(B) Three-dimensional reconstruction of apo-PhPFD, showing the same orthogonal views. Flexible docking of the atomic structure of MtPFD (Siegert et al., 2000) (PDB accession number 1FXK) is shown in ribbon style inside the electron microscopy map. Greek letters point to the subunits that form part of the PhPFD oligomer.

Archaeal PFD Uses Its Tentacles Tips to Dock atop the Thermosome Cavity

Chaperonins are one of the few molecular chaperones present in all three domains of life. The least understood chaperonins (“thermosomes”) are from archaea, where little is known about their *in vivo* folding abilities (Gutsche et al., 1999). The thermosomes reveal, unlike their eubacterial and eukaryotic counterparts, variability both in symmetry (8- or 9-fold symmetry) and composition (one to three different subunits). The *P. horikoshii* thermosome (PhTherm) is a homo-oligomer of unknown symmetry but under the electron microscope, reveals the two typical views described for all chaperonins (Okochi et al., 2005). In the case of the end-on view, the average image we obtained from 1425 particles (Figure 2A) reveals a doughnut-shaped structure with clear 8-fold symmetry, indicating that PhTherm is an octameric ring. The averaging of 2524 particles of the side view confirms the presence of a dual stacked ring structure (Figure 2B), with dimensions of ~168 Å long by ~158 Å wide.

It has been shown that the chaperone PFD releases its substrate into the chaperonin cavity via a physical, albeit transient, interaction between the two chaperones (Vainberg et al., 1998; Siegers et al., 1999). In eukaryotes, this interplay has been confirmed by a three-dimensional reconstruction of the complex between human PFD and the chaperonin CCT (Martín-Benito et al., 2002). In archaea, the interaction between the two chaperones has been characterized, but only by using biophysical techniques (Okochi et al., 2004; Zako et al., 2005). Here, we examined the interaction between PhTherm and PhPFD by electron microscopy. Incubation of both chaperones at different conditions generated in all cases a small percentage of PhTherm:PhPFD complexes, perhaps reflecting the transient nature of the interaction. This prevented a three-dimensional reconstruction from being carried

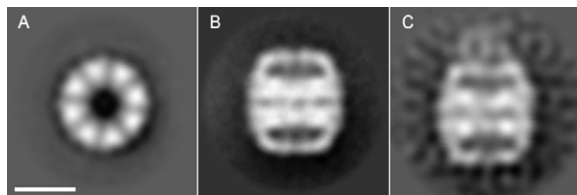


Figure 2. Structural Characterization of the PhTherm and PhTherm-PhPFD Interaction

(A) Two-dimensional average image of the end-on view of PhTherm. (B) Two-dimensional average image of the side view of the PhTherm. (C) Two-dimensional average image of the side view of the PhTherm:PhPFD complex. Bar represents 100 Å.

out by cryo-electron microscopy. Nevertheless, the two-dimensional average image of the PhTherm:PhPFD complex generated from 608 particles shows the interaction occurring between the tips of PhPFD tentacles and the interior of the thermosome apical domains (Figure 2C), which is in agreement with biochemical data that the tips of the tentacles are responsible of the interaction between PhTherm and PhPFD (Okochi et al., 2005). An interesting observation is that the tentacles of PhPFD do not penetrate in the thermosome cavity as much as those of the eukaryotic PFD into the CCT cavity. This was observed in the latter case by using both negatively stained and frozen-hydrated preparations (see Figures 3D–3F of Martín-Benito et al. [2002]), and although the unstained average image (Figure 3F of Martín-Benito et al. [2002]) reveals more faithful details than its negatively stained counterparts (Figures 3D and 3E of Martín-Benito et al. [2002]), in all cases, the average images seem to penetrate more in the eukaryotic chaperonin than in the case of PhPFD with regard to PhTherm (Figure 2C). We believe that this difference may have important consequences in the substrate transfer mechanism between the two types of PFDs and their corresponding chaperonins (see below).

Another important difference between the two types of PFDs is that unlike the eukaryotic one, which can bind one or both rings of CCT simultaneously (Martín-Benito et al., 2002), PhPFD was only observed to form asymmetric complexes with PhTherm. This suggests a different behavior in both chaperonins with respect to the interring allosteric communications induced by the PFD interaction.

The Multivalent and Differential Interaction of PhPFD with Varying Unfolded Proteins

Biochemical studies performed with several archaeal PFDs suggest for these chaperones a promiscuous role in the stabilization and delivery of unfolded proteins to their corresponding thermosomes (Leroux et al., 1999; Lundin et al., 2004; Okochi et al., 2002). Unlike eukaryotic PFD, which has only been shown to interact directly with nonnative actin and tubulin, archaeal PFDs appear to bind denatured proteins indiscriminately, either mesophilic or thermophilic substrates (Gutsche et al., 1999). We therefore sought to visualize directly how PhPFD interacts with substrates of different sizes and structures. We

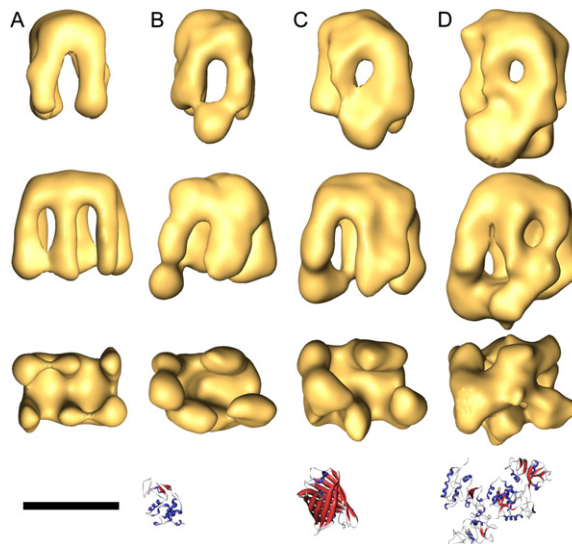


Figure 3. Three-Dimensional Reconstruction of the Complex between PhPFD and Several Unfolded Proteins

(A) Three orthogonal views of the three-dimensional reconstruction of apo-PhPFD.

(B–D) The same views of the three-dimensional reconstructions of PhPFD complexed to unfolded lysozyme (B), GFP (C), and conalbumin (D). The bottom images correspond respectively to the atomic structures of lysozyme, GFP, and conalbumin, at the same scale. Note that the native structures of the substrates are shown only for relative size and shape comparisons and are not intended to represent the actual conformations of the nonnative proteins bound to PhPFD. Bar represents 50 Å.

chose as substrates denatured forms of the mostly α -helical lysozyme (14 kDa), the medium-size green fluorescent protein (GFP; 27 kDa) that is composed mostly of β strands, and the large, α/β protein conalbumin (75 kDa). The three proteins were denatured with a chaotrope and independently incubated with PhPFD. Aliquots of the complexes formed were subsequently stained with 2% uranyl acetate, and particles were selected and used for the three-dimensional reconstruction of the PhPFD:lysozyme, PhPFD:GFP, and PhPFD:conalbumin complexes (3158, 3241, and 3173 particles, respectively). In all three cases (Figure 3), the volumes generated reveal the typical structure of PFD obtained so far, namely a structure with six tentacles hanging from a rectangular base. However, unlike the three-dimensional reconstruction of the apo-PhPFD (Figure 3A), the volumes of the PhPFD:lysozyme (Figure 3B), PhPFD:GFP (Figure 3C), and PhPFD:conalbumin (Figure 3D) complexes reveal a stain-excluding mass interacting with the tip of some of the PhPFD tentacles. The masses of each unfolded protein protrude from the PhPFD cavity, and their sizes are consistent with that of their corresponding native structures (see atomic structures in Figure 3). The volumes reconstructed also reveal that the number of PhPFD subunits coiled coils involved in the interaction with the unfolded substrates increases with the size of the denatured protein (see the bottom views for each of the three-dimensional reconstructions).

Accordingly, lysozyme interacts with a pair of PhPFD β subunits (Figure 3B), GFP binds to a pair of PhPFD β subunits plus one of the PhPFD α subunits (Figure 3C), and the largest protein, conalbumin, interacts with all six PhPFD subunits (Figure 3D). The arrangement of the tentacles in the PhPFD:substrate complexes (Figures 3B–3D) seems to deviate from the position of the apo-PhPFD tentacles (Figure 3A), which suggests a flexing of the coiled coils to accommodate the interaction with substrates of different size and shape.

To confirm biochemically these structural results, we generated PhPFD mutants with truncations of the N and C termini for both PhPFD α and PhPFD β subunits, which correspond topologically to the tips of the chaperone tentacles and subsequently tested their interaction with different substrates. For GFP, it was previously shown by truncation analysis that the PhPFD β subunits are important for substrate binding activity, whereas the PhPFD α subunits are less critical (Okochi et al., 2004), which agrees with the structural data shown here. To further dissect the relative contribution of each tentacle to binding different proteins, we tested nonnative lysozyme and conalbumin as substrates. The two proteins were chemically denatured, and their aggregation upon dilution was assayed in the absence or presence of either wild-type PhPFD or the following deletion mutants: an N- and C-terminal truncation in the PhPFD α subunits (15 and 21 residues, respectively; PhPFD α Tr), another mutant with comparable truncation in the PhPFD β subunits (13 residues in both N- and C-terminal domains; PhPFD β Tr), or a mutant with truncations in both subunits (PhPFD α Tr β Tr) (Figures 4A and 4C). The results obtained show that in the case of lysozyme, removal of the PhPFD α tips results in a small decrease in the prevention of aggregation, as compared to wild-type PhPFD (Figure 4A), consistent with our demonstration that only PhPFD β subunits are involved in the interaction with lysozyme (Figure 3B). Unexpectedly, however, the activity of the chaperone with truncated PhPFD β subunits is not completely abolished (Figure 4A). This apparent paradox could be explained if the PhPFD α subunits substitute for the PhPFD β ones in the stabilization of the unfolded protein once the tips of the latter are removed. Indeed, this is what happens, as revealed by a three-dimensional reconstruction of the complex formed between PhPFD β Tr and unfolded lysozyme (2729 particles analyzed) (Figure 4B), which shows the mass of the unfolded lysozyme interacting with the centrally positioned pair of PhPFD α subunits compared with the peripheral PhPFD β subunits in the wild-type complex (Figure 3B). At this stage, it is unclear whether the somewhat different shapes of the unfolded lysozyme bound to PhPFD (Figure 3B) or PhPFD β Tr (Figure 4B) stems from the relatively low resolving power of the three-dimensional reconstructions or reflects the stabilization of an alternate form of unfolded lysozyme between the two types of PhPFD subunits.

When the same prevention-of-aggregation experiments were performed with denatured conalbumin (Figure 4C), we observed that removal of the PhPFD α tips only slightly

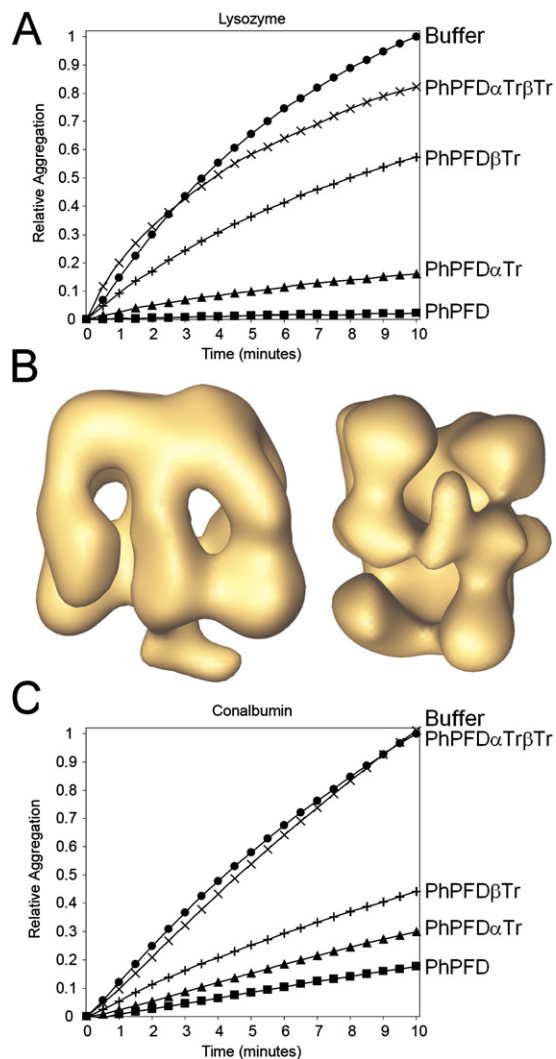


Figure 4. The Role of PhPFD α and PhPFD β Subunits in the Interaction with Unfolded Substrates

(A) Effect of truncating the tips of PhPFD α and PhPFD β subunits in preventing the aggregation of denatured lysozyme. Relative aggregation, as defined by detecting light scattering spectrophotometrically at 360 nm, was monitored over a period of 10 min.

(B) Two orthogonal views of the three-dimensional reconstruction of the complex between PhPFD β Tr and unfolded lysozyme.

(C) Effect of truncation of the tips of PhPFD α and PhPFD β subunits in preventing the aggregation of denatured conalbumin.

reduces the ability of the chaperone to prevent aggregation, and truncation of the PhPFD β tips alone resulted in only a further small increase in the aggregation of the nonnative protein. Only the truncation of both of the PhPFD α and PhPFD β tips abolish PhPFD protection of conalbumin aggregation (Figure 4C). These data clearly indicate that all six PhPFD subunits are used in the stabilization of unfolded conalbumin, a finding consistent with mutagenesis data showing that archaeal PFD α and PFD β coiled-coil tentacles act synergistically to stabilize nonnative proteins (Lundin et al., 2004). In addition, the results confirm our observation that all PFD subunit tentacles are engaged

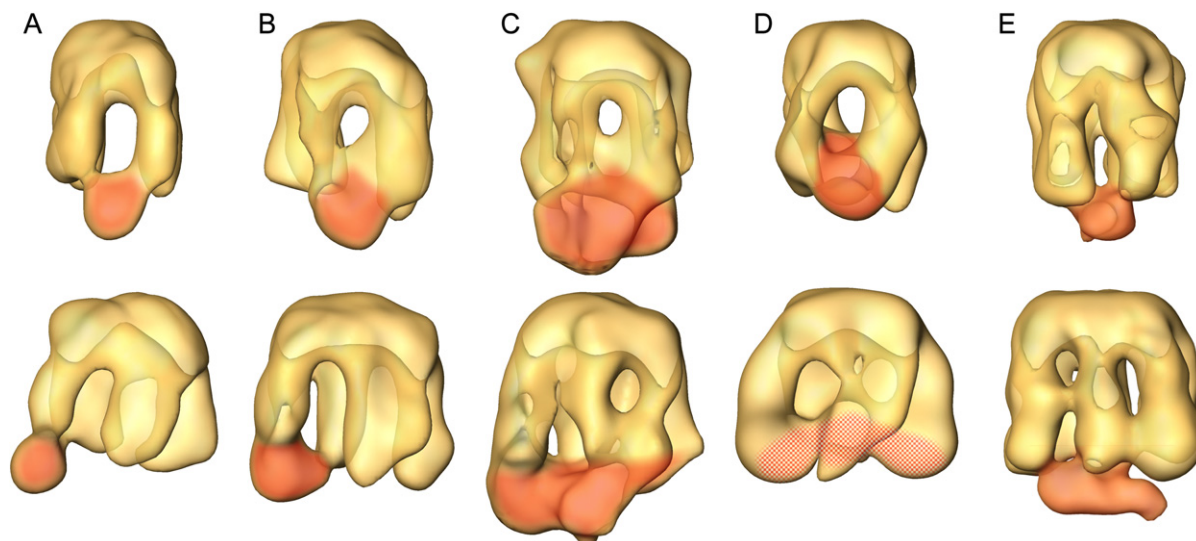


Figure 5. Localization of the Unfolded Substrates in Archaeal and Eukaryotic PFDs

(A–C) Two orthogonal views of the three-dimensional reconstruction of the complex between PhPFD and unfolded lysozyme (A), GFP (B), and conalbumin (C).

(D) The same two views of the three-dimensional reconstruction of the complex between human PFD and unfolded actin.

(E) The same two views of the three-dimensional reconstruction of the complex between PhPFD and unfolded actin. In all cases, the unfolded protein is depicted in red, except in (D [bottom]), which is colored in light red to indicate that the mass of the unfolded actin is enclosed in, and obscured by, the chaperone cavity.

in the PhPFD:conalbumin complex observed by electron microscopy (Figure 3D).

Interaction versus Encapsulation: A Different Behavior in the Substrate-Binding Mechanism between the Archaeal and Eukaryotic PFD

An interesting observation is that the three unfolded substrates studied here interact with PhPFD without being encapsulated in the cavity formed by the six PhPFD tentacles (Figures 5A–5C). This is surprising since the interaction observed previously between the eukaryotic PFD and unfolded actin revealed the mass of the cytoskeletal protein inserted and protected in the PFD cavity (Martin-Benito et al., 2002) (Figure 5D). This suggests a different substrate-binding mechanism between the archaeal and eukaryotic PFDs. To test this possibility, we denatured actin with a chaotropic agent, incubated it with PhPFD, and selected 2812 particles to generate a three-dimensional reconstruction of the complex (Figure 5E).

The volume obtained reveals the unfolded actin as a mass not encapsulated in the PhPFD cavity but instead protruding from it, similar to that seen with unfolded GFP or conalbumin, with several PhPFD tentacles contacting the client protein. This finding confirms the difference in the substrate-binding mechanisms of archaeal and eukaryotic PFD. Furthermore, the cylindrical shape of the unfolded actin bound to the archaeal chaperone is comparable to that seen in the eukaryotic PFD-actin or chaperonin CCT-actin complexes (Llorca et al., 1999; Martin-Benito et al., 2002), which strengthens the notion that actin reaches a considerable degree of secondary structure by itself before interacting with the chaperones (Schüler et al., 2000).

DISCUSSION

The archaeal PFDs have been shown to interact with a wide range of substrates, protecting them from unwanted interactions and delivering them into the chaperonin cavity (Gutsche et al., 1999; Leroux et al., 1999; Lundin et al., 2004; Zako et al., 2005). The results described here illustrate the promiscuity of this chaperone in the interaction with unfolded proteins, since a stable interaction takes place between PhPFD and three proteins of different size and secondary structure: lysozyme, a small protein (14 kDa) of mostly α -helical nature; GFP, a protein of medium size (27 kDa) that forms a β -barrel in its native conformation, and conalbumin, an α/β protein of large size (75 kDa). In all three cases, the unfolded proteins seem to have reached a certain degree of compactness before interacting with PhPFD. The interplay between archaeal PFDs and the unfolded proteins seems to occur through a set of hydrophobic residues involved in interhelical contacts in the coiled coils and located at the tips of the chaperone tentacles (Siegert et al., 2000; Lundin et al., 2004; Okochi et al., 2004). Our electron microscopy reconstructions of the complexes formed between PhPFD and various substrates confirm this type of interaction (Figure 3). Curiously enough, and despite the fact that the tips of both PhPFD α and PhPFD β subunits expose hydrophobic residues in their inner surface (Lundin et al., 2004), the tips of one of the PhPFD β pairs are always involved in binding the unfolded proteins. A small protein-like lysozyme (14 kDa) only requires such an interaction (Figure 3B), whereas larger substrates require binding to additional PhPFD subunits (Figures 3C and 3D). This structural

observation confirms the deletion experiments performed on several archaeal PFDs, including *P. horikoshii*, which reveal that PhPFD β subunits are more important than the neighboring PhPFD α subunits for stabilizing unfolded proteins (Siegert et al., 2000; Lundin et al., 2004; Okochi et al., 2004). As discussed below, this preference for PFD β subunits may play a role in the substrate transfer mechanism to the thermosome.

The three-dimensional structures of PhPFD complexed to three unfolded proteins reveal a structural plasticity of the archaeal chaperone since its tentacles deviate from the structure obtained in the apo-PhPFD to accommodate the denatured proteins (Figure 3). This finding is remarkable because, to our knowledge, it shows for the first time that the jellyfish-like architecture and flexibility of archaeal PFD is ideally suited for interacting with a diverse array of nonnative proteins with different sizes and shapes. Even more interesting is our observation that the three unfolded proteins are not confined inside the cavity formed by the PhPFD tentacles but rather protrude from it (Figures 5A–5C). This is a surprising result, given that in the three-dimensional reconstruction of the eukaryotic PFD:unfolded actin complex (Martín-Benito et al., 2002), the cytoskeletal protein is found almost entirely encapsulated in the rectangular chaperone cavity (Figure 5D). The difference in localization cannot be ascribed to substrate sizes, as actin has a molecular mass (42 kDa) intermediate between that of GFP (27 kDa) and conalbumin (75 kDa), both of which are nearly excluded from the archaeal PFD cavity (Figure 3). The three-dimensional reconstruction of a complex between the archaeal PhPFD and the unfolded, eukaryotic actin reveals the mass of the cytoskeletal protein not confined in the chaperone cavity but rather interacting with the tips of several PhPFD tentacles (Figure 5E), confirming a clear difference in the mechanism of substrate interaction between archaeal PFD and its eukaryotic counterpart. This suggests a distinct role for the two types of chaperones that might have originated when the simpler archaeal-like PFD evolved toward a structure with a more complex subunit composition. Indeed, the divergence in PFD function correlates with the evolution of the group II-type chaperonins that they serve (Leroux and Hartl, 2000). Whereas archaeal chaperonins and PFDs are composed respectively of one to three and two types of subunits, the eukaryotic cytosolic chaperonin CCT and PFD are composed respectively of eight and six different subunits. This coevolution toward a higher complexity correlates with a specialization in the function of both chaperonins and PFDs; thus, whereas the archaeal PFDs and chaperonins seem to act on a variety of substrates (Gutsche et al., 1999; Leroux et al., 1999; Leroux and Hartl, 2000), the eukaryotic PFD and CCT has been shown to be mostly involved in the folding of a more limited set of substrates, including two (actins and tubulins) that are restricted to the eukaryal domain (Vainberg et al., 1998; Geissler et al., 1998; Siegers et al., 2003; Valpuesta et al., 2005).

The evolution of PFDs in terms of structure and specialization seems to be associated with a change in their

function, from an archaeal chaperone that traps and thus stabilizes unfolded proteins until their transfer to the thermosome to an eukaryotic one that recognizes a certain set of unfolded proteins (i.e., actins and tubulins) and shields them in its cavity until their transfer to CCT. This protective role of the eukaryotic PFD is so important that its presence increases by at least 5-fold the amount of actin folded by CCT in vivo (Siegers et al., 1999). The change in the role of PFD, from a stabilizer and carrier in the archaeal PFDs to a more specialized, protective role for the eukaryotic PFDs, must be accompanied by changes in the mechanism of substrate recognition and interaction. Therefore, whereas the recognition mechanism in archaeal PFDs relies on nonspecific, hydrophobic interactions (Siegert et al., 2000; Lundin et al., 2004; Okochi et al., 2004) (Figure 6A), the eukaryotic PFDs have evolved more specific interactions based on particular sequences in the chaperone and the unfolded protein (Figure 6D). This has been shown for the cytoskeletal proteins β -actin, α -, β -, γ -tubulin, and actin-related protein ARP-1 (Romme-laere et al., 2001), which seem to possess at least two identifiable PFD-binding sites in their sequence, one of them sharing a common binding motif. Likewise, truncation experiments in the subunits of human PFD reveal specific domains for interaction with tubulin and actin (Torrey-Simons et al., 2004).

The three-dimensional structures of the eukaryotic and archaeal PFDs complexed to unfolded proteins (Martín-Benito et al., 2002; this work) give some insight into the two roles of this chaperone, the interaction with unfolded proteins and their delivery into the chaperonin for subsequent folding. We show that, as with eukaryotic PFD, the archaeal counterpart uses its coiled-coil tips to bind directly at the entrance of the chaperonin cavity (Figure 2). Thus, both the eukaryal and archaeal PFDs interact with their corresponding chaperonin to deliver an unfolded polypeptide. The topology of this interaction suggests to us a different mechanism of interaction between the archaeal and eukaryotic systems with regard to the interaction of the PFDs with their corresponding chaperonins. Whereas PhPFD uses its coiled-coil tips to interact with the thermosome apical domains (Figure 2C), the eukaryotic PFD inserts its tips in the cavity of the chaperonin CCT (Figures 3D–3F in Martín-Benito et al. [2002]). Since the unfolded proteins interact with PhPFD outside the chaperone cavity, whereas unfolded actin is encapsulated inside the cavity of the eukaryotic PFD, the delivery of substrate may in both cases occur near the same region of the chaperonin apical domain. This is however speculative and further experiments would be needed to prove the differences in the interaction mechanism between the two types of chaperones.

In any case, the delivery of the unfolded protein from the PFD chaperone to its corresponding chaperonin could take place simultaneously with binding, which is supported by the fact that, as shown biochemically (Siegert et al., 2000; Okochi et al., 2004) and structurally (Martín-Benito et al., 2002; this work), the tips of the PFD tentacles are involved in the interaction with both the chaperonin

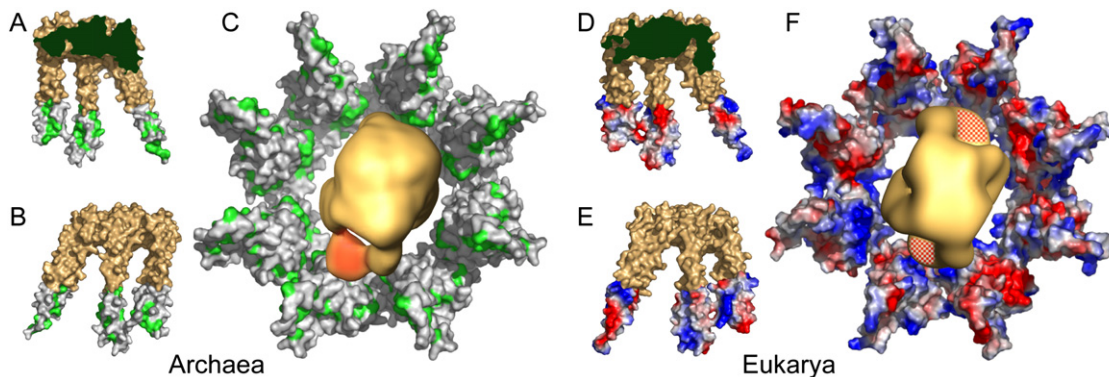


Figure 6. Model of Substrate Transfer from PFD to Its Corresponding Chaperonin

(A and B) Views from the interior and exterior, respectively, of the atomic model of the PhPFD $\beta\alpha\beta$ trimer. The atomic model was generated with the MtPFD atomic structure, as described in the [Experimental Procedures](#) section, and the residues colored green correspond to the hydrophobic residues located in the tips of the PhPFD subunits.

(C) A model of substrate transfer from PhPFD to PhTherm as seen from the entrance of the chaperonin cavity. The atomic model of the open conformation of the PhTherm was generated as described in the [Experimental Procedures](#) section. The volume of PhPFD located in the center of the chaperonin cavity is that of the three-dimensional reconstruction of the complex formed between PhPFD and the unfolded lysozyme (the latter depicted in orange).

(D and E) Views from the interior and exterior, respectively, of the atomic model of the human PFD. In the model, only the trimer corresponding to subunits PFD2, PFD3, and PFD4 is depicted. The residues colored red and blue correspond to the acidic and basic residues located at the tips of these three PFD subunits.

(F) A model of substrate transfer from human PFD to the eukaryotic chaperonin CCT, as seen from the entrance of the chaperonin cavity. The model of the open conformation of CCT with its eight different subunits was generated as described in the [Experimental Procedures](#) section. The residues colored red and blue in the CCT structure correspond to the acidic and basic residues located in the inner side of the apical domains of the chaperonin. The volume of PFD located in the center of the chaperonin cavity is that of the three-dimensional reconstruction of the complex formed between human PFD and the unfolded actin ([Martín-Benito et al., 2002](#)), and the mass corresponding to the actin mass that protrudes from the chaperone cavity is colored red. The interaction between the PFD:actin complex and CCT has been placed at random, without any attempt to indicate a precise interaction between PFD and CCT, and for this reason, the CCT subunits are not labeled.

and the unfolded protein. In the case of the archaeal system, the biochemical and structural results shown here and elsewhere ([Sieger et al., 2000](#); [Okochi et al., 2004](#)) reveal that the PhPFD β subunits are most important with regard to interaction with unfolded proteins and with PhTherm, which takes place in this case through the outer regions of the tips of the PhPFD β tentacles ([Okochi et al., 2004](#)) (Figures 2C and 6B). Together, these observations suggest a simple substrate transfer mechanism by which the outer regions of the PhPFD β tips (Figure 6B) interact with a ring of hydrophobic residues located at the entrance of the thermosome cavity and present the unfolded protein to the same ring of residues (Figure 6C). Since PhTherm is composed of eight identical subunits, there must be eight equivalent positions for such an interaction (Figure 6C). In the case of the eukaryotic PFD, the topology of interaction between the two chaperones must be similar, and therefore it is very likely that the four outer PFD β -like subunits ([Torrey-Simons et al., 2004](#)) (PFD1, PFD2, PFD4, and PFD6) are more involved than the central PFD α -like ones (PFD3 and PFD5) in such an interplay. However, unlike its archaeal counterpart, the interaction between the two eukaryotic chaperones must rely on specific residues located in the outer region of the tips of the PFD tentacles (Figure 6E) and in the apical domains of specific CCT subunits, leading to a single, unique type of interaction (Figure 6F). This unique interaction has been shown to exist, since the three-dimensional reconstruction of the

complex between CCT and two human PFDs reveal only one type of interaction (see Figure 4E in [Martín-Benito et al. \[2002\]](#)), but the nature of the specific PFD-CCT subunit interactions taking place has yet to be discovered.

In summary, our structural and biochemical studies on the interaction between PFD and its cognate chaperonin and different substrates reveal that the mechanism of functional cooperation between PFD and chaperonin is remarkably conserved and, at the same time, suggest a striking difference in the mode of substrate binding between archaeal and eukaryotic PFD that is respectively consistent with general and specialized roles in cellular protein folding. Our findings therefore offer structural and functional insights into the coevolution of the archaeal PFD-chaperonin system toward one in eukarya capable of facilitating the folding of two classes of proteins—actins and tubulins—that were essential in the emergence of a cytoskeleton that can support the more complex processes that define eukaryotic cells.

EXPERIMENTAL PROCEDURES

Cloning, Overexpression, and Purification of the Thermosome and the Various PFD Oligomers from *Pyrococcus horikoshii*

The coding sequence of the *P. horikoshii* thermosome gene (PH0017) was amplified by PCR with chromosomal DNA from *P. horikoshii* (ATCC 700860) as template and two oligonucleotides (5'-GTTCATA TGGCATTAGCA-3'/5'-CCGGATCCACTTCAGTCTAG-3') containing NdeI and BamHI restriction sites as primers (underlined). The

amplified 1650 bp fragment was inserted into the pCR2.1 plasmid (Invitrogen) and then cloned in the NdeI/BamHI restriction sites of pET22b(+) (Invitrogen) to obtain the expression plasmid pET22TPH. For the overexpression of the prefoldin under the control of the T7-dependent promoter, a synthetic bicistronic β - α operon was constructed in two steps. First, the gene coding for the PhPFD β subunit (PH0532) was amplified from the same template with a pair of oligonucleotides (primers 5'-CATATGCAGAACATTCTCC-3' and 5'-AAAG AAGAGGTCAGCCAG-3'; the NdeI site is underlined), and the 354 bp PCR product obtained was subsequently cloned into pCR2.1. The gene was purified from this intermediate by NdeI/EcoRI digestion, and cloned into the same restriction sites of pET22b(+), leading to pET22 β . In a second step, the gene coding for the PhPFD α subunit (PH0527) and its Shine-Dalgarno sequence was also amplified with primers 5'-GAAATTCAACTTTAAGAAGGAGATAT-3' and 5'-CTCGAGC TACTTCTTAACCTAAAG-3' (EcoRI and XhoI sites are underlined), and after an intermediate cloning into pCR2.1 of the 449 bp PCR product, it was inserted into the EcoRI/NdeI sites of pET22 β , leading to the final expression plasmid pET22 $\beta\alpha$.

For the cloning of the PhPFD truncations, PCR mutagenesis with internal primers was used to remove the N and C termini of the wild-type PhPFD α and PhPFD β subunits. The truncations were designed to leave a flush end maintaining the coiled-coil structure of the tentacle for both PhPFD β Tr (amino acids 13–104 remaining) and PhPFD α Tr (amino acids 15–130 remaining). The truncated and wild-type subunits were expressed as in Lundin et al. (2004).

Overproduction of the thermosome and PhPFD from the corresponding expression vectors was carried out in *E. coli* BL21(DE3). Bacteria were grown at 37°C in LB to an OD₅₅₀ = 0.3 before addition of 0.1 mM IPTG (Isopropyl- β -D-thiogalactopyranoside). Four hours later, the cells were harvested by centrifugation. Purification of PhPFD was carried out essentially as described by Okochi et al. (2002). Overexpression and purification of the truncated forms of PhPFD was carried out as described by Lundin et al. (2004). Purification of PhTherm was carried out as previously described (Yoshida et al., 2001) for the purification of the *Thermococcus* strain KS-1 thermosome.

Aggregation Assays

Lysozyme (200 μ M) or conalbumin (75 μ M) were denatured in 6 M guanidine-HCl, 100 mM NaCl, 20 mM sodium phosphate, 50 mM DTT (pH 8.0). Denatured substrates were diluted 100-fold into buffer (20 mM sodium phosphate, 100 mM NaCl [pH 8.0]) or buffer containing wild-type or truncated PFD. For lysozyme, the various PhPFD complexes were at 2 μ M and for conalbumin the complexes were at 3.75 μ M. The absorbance change was monitored at 360 nm for 10 min, and the data was analyzed as previously described (Lundin et al., 2004).

Formation of PhTherm:PhPFD and PhPFD:substrate Complexes

For electron microscopy, the PhTherm:PhPFD complexes were generated by incubating a 15 M excess of PhPFD over PhTherm (0.2 μ M final concentration). In the case of the complexes formed by PhPFD and the unfolded proteins lysozyme, GFP, conalbumin, and actin, they were subjected to chemical denaturation. GFP was denatured by acid treatment, as described (Lundin et al., 2004), whereas in the case of lysozyme, conalbumin, and actin, their denaturation was accomplished by a 6 M guanidium chloride treatment. After denaturation, the unfolded proteins were diluted 50-fold in a buffer containing PhPFD so that the PhPFD:unfolded protein ratio is 1:1 (5 μ M PhPFD final concentration).

Electron Microscopy

For each sample (PhTherm, PhPFD, and PhPFD complexed to either PhTherm or various substrates), 5 μ l aliquots were applied to glow-discharged carbon grids for 1 min and then stained for 1 min with 2% uranyl acetate. Images were recorded at 0° tilt in a JEOL 1200EX-II electron microscope operated at 100 KV and recorded at 60,000 \times nominal magnification.

Image Processing, Two-Dimensional Averaging, and Three-Dimensional Reconstruction

Micrographs were digitized in a Zeiss SCAI scanner with a sampling window corresponding to 2.8 Å/pixel. For two-dimensional classification and averaging of PhTherm or PhTherm:PhPFD complexes, particles were selected and processed by using a free-pattern, maximum-likelihood multireference refinement (Scheres et al., 2005).

The three-dimensional reconstruction of apo-PhPFD was generated from negatively stained, randomly oriented particles, using the EMAN package for single-particle three-dimensional reconstruction (Ludtke et al., 1999). The initial volume was generated by the common-line procedure included in the EMAN package, with the average classes obtained after multivariate statistical analysis. A 2-fold symmetrization was imposed on the volumes generated throughout the iterative process. The final resolution was estimated to be 19 Å with the 0.5 criterion for the Fourier shell correlation coefficient between two independent reconstructions. For the three-dimensional reconstructions of the PhPFD:lysozyme, PhPFD β Tr:lysozyme, PhPFD:GFP, PhPFD:conalbumin, and PhPFD:actin complexes, the corresponding particles were subjected to the reconstruction procedure described above, except that the volume of the apo-PhPFD was used as the reference volume and that no symmetry was imposed throughout the reconstruction process. The final resolutions for the PhPFD:lysozyme, PhPFD β Tr:lysozyme, PhPFD:GFP, PhPFD:conalbumin, and PhPFD:actin complexes were 20, 20, 21, 22, and 19 Å, respectively. The red color used in Figure 5 to indicate the localization of the unfolded substrate was assigned empirically. Docking of the atomic structure of MtPFD (PDB code 1FXK) into the three-dimensional electron microscopy map of apo-PhPFD was performed by the flexible docking algorithm included in the SITUS package (Wriggers et al., 2004). Visualization of the volumes was carried out with AMIRA (<http://www.amiravis.com/>).

Generation of the Atomic Models

The atomic models of PhPFD and the human PFD were generated with the atomic structure of MtPFD as template. Atomic models of PhTherm and CCT were generated with *Thermoplasma acidophilum* (Ditzel et al., 1998) (PDB code 1A6D) and mouse CCT γ (Pappenberger et al., 2002) (PDB code 1GML) structures as templates and modified to approximately fit into the three-dimensional reconstruction of the structure of nucleotide-free CCT obtained by cryoelectron microscopy (Llorca et al., 2000), essentially as described elsewhere (Gomez-Puertas et al., 2004). All atomic models were constructed by homology modeling procedures based on multiple structure-based amino acid sequence alignments of the homologous proteins of the PFD or thermosome/CCT families, extracted from the Pfam database (Bateman et al., 2004). Atomic models were built with the SWISS-MODEL server facilities (Schwede et al., 2003), and their structural quality was checked with the WHAT-CHECK routines (Hoof et al., 1996) from the WHAT IF program (Vriend, 1990). Finally, in order to optimize geometries and correct possible bad contacts, the obtained models were refined by subjecting them to three steps of 50 cycles of steepest descent minimization method implemented in the program DeepView (Guex and Peitsch, 1997). Atomic surfaces were generated with Pymol (DeLano Scientific, San Carlos, CA), and electrostatic potentials were calculated with GRASP (Nicholls et al., 1991).

ACKNOWLEDGMENTS

We thank Hugo Yébenes for his technical assistance. This work was supported by grants BFU2004-00232 (J.M.V.), BIO2004-02671 (J.B.), SAF2004-06843 (P.G.P.), as well as by CIHR (BMA121093) to M.R.L. M.R.L. holds Michael Smith Foundation for Health Research and Canadian Institutes of Health Research scholarships, and P.C.S. is supported by Natural Sciences and Engineering Research Council of Canada and Michael Smith Foundation for Health Research scholarships. This work was also supported by the EU-grant "3D repertoire" (LSHG-CT-2005-512028) and by the grant RGP63/2004 from the Human Frontiers Scientific Program.

Received: October 17, 2006
 Revised: November 28, 2006
 Accepted: November 28, 2006
 Published: January 16, 2007

REFERENCES

- Bateman, A., Coin, L., Durbin, R., Finn, R.D., Hollich, V., Griffiths-Jones, S., Khanna, A., Marshall, M., Moxon, S., Sonnhammer, E.L., et al. (2004). The Pfam protein families database. *Nucleic Acids Res.* 32, D138–D141.
- Bukau, B., and Horwich, A.L. (1998). The hsp70, hsp60 chaperone machines. *Cell* 92, 351–366.
- Ditzel, L., Löwe, J., Stock, D., Stetter, K.O., Huber, H., Huber, R., and Steinbacher, S. (1998). Crystal structure of the thermosome, the archaeal chaperonin and homologue of CCT. *Cell* 93, 125–138.
- Ellis, R.J., and Hartl, F.U. (1999). Principles of protein folding in the cellular environment. *Curr. Opin. Struct. Biol.* 9, 102–110.
- Geissler, S., Siegers, K., and Schiebel, E. (1998). A novel protein complex promoting formation of functional alpha- and gamma-tubulin. *EMBO J.* 17, 952–966.
- Gomez-Puertas, P., Martin-Benito, J., Carrascosa, J.L., Willison, K.R., and Valpuesta, J.M. (2004). The substrate recognition mechanisms in chaperonins. *J. Mol. Recognit.* 17, 85–94.
- Guex, N., and Peitsch, M.C. (1997). SWISS-MODEL and the Swiss-PdbViewer: an environment for comparative protein modelling. *Electrophoresis* 18, 2714–2723.
- Gutsche, I., Essen, L.O., and Baumeister, W. (1999). Group II chaperonins: new TRiC(k)s and turns of a protein folding machine. *J. Mol. Biol.* 293, 295–312.
- Hansen, W.J., Cowan, N.J., and Welch, W.J. (1999). Prefoldin-nascent chain complexes in the folding of cytoskeletal proteins. *J. Cell Biol.* 145, 265–277.
- Hooft, R.W., Vriend, G., Sander, C., and Abola, E.E. (1996). Errors in protein structures. *Nature* 381, 272.
- Leroux, M.R., and Hartl, F.U. (2000). Protein folding: versatility of the cytosolic chaperonin TRiC/CCT. *Curr. Biol.* 10, R260–R264.
- Leroux, M.R., Fandrich, M., Klunker, D., Siegers, K., Lupas, A.N., Brown, J.R., Schiebel, E., Dobson, C.M., and Hartl, F.U. (1999). MtGimC, a novel archaeal chaperone related to the eukaryotic chaperonin cofactor GimC/prefoldin. *EMBO J.* 18, 6730–6743.
- Llorca, O., McCormack, E.A., Inés, G., Grantham, J., Cordell, J., Carrascosa, J.L., Willison, K.R., Fernández, J.J., and Valpuesta, J.M. (1999). Eukaryotic type II chaperonin CCT interacts with actin through specific subunits. *Nature* 402, 693–696.
- Llorca, O., Martín-Benito, J., Ritco-Vonsovici, M., Grantham, J., Hynes, G., Willison, K.R., Carrascosa, J.L., and Valpuesta, J.M. (2000). Eukaryotic chaperonin CCT stabilizes actin and tubulin folding intermediates in open quasi-native conformations. *EMBO J.* 19, 5971–5979.
- Ludtke, S.J., Baldwin, P.R., and Chiu, W. (1999). EMAN: semi automated software for high-resolution single-particle reconstructions. *J. Struct. Biol.* 128, 82–97.
- Lundin, V.F., Stirling, P.C., Gómez-Reino, J., Kim, P.-B., Mwenifumbo, J.C., Obst, J.M., Valpuesta, J.M., and Leroux, M.R. (2004). Molecular clamp mechanism of substrate binding by hydrophobic coiled coil residues in the archaeal chaperone, prefoldin. *Proc. Natl. Acad. Sci. USA* 101, 4367–4372.
- Martín-Benito, J., Boskovic, J., Gómez-Puertas, P., Carrascosa, J.L., Simons, C., Lewis, S.A., Bartolini, F., Cowan, N.C., and Valpuesta, J.M. (2002). Structure of eukaryotic prefoldin and of its complexes with unfolded actin and the cytosolic chaperonin CCT. *EMBO J.* 21, 6377–6386.
- Mogk, A., Bukau, B., and Deuerling, E. (2001). Cellular functions of cytosolic *E. coli* chaperones. In *Molecular Chaperones in the Cell*, P. Lund, ed. (Oxford, UK: Oxford University Press), pp. 3–34.
- Nicholls, A., Sharp, K.A., and Honig, B. (1991). Protein folding and association: insights from the interfacial and thermodynamic properties of hydrocarbons. *Proteins* 11, 281–296.
- Okochi, M., Yoshida, T., Maruyama, T., Kawarabayashi, Y., Kikuchi, H., and Yohda, M. (2002). Pyrococcus prefoldin stabilizes protein-folding intermediates and transfers them to chaperonin for correct folding. *Biochem. Biophys. Res. Commun.* 297, 769–774.
- Okochi, M., Nomura, T., Zako, T., Arakawa, T., Iizuka, R., Ueda, H., Funatsu, T., Leroux, M., and Yohda, M. (2004). Kinetics and binding sites for interaction of prefoldin with group II chaperonin: contiguous non-native substrate and chaperonin binding sites in archaeal prefoldin. *J. Biol. Chem.* 279, 31788–31795.
- Okochi, M., Matsuzaki, H., Nomura, T., Ishii, N., and Yohda, M. (2005). Molecular characterization of the group II chaperonin from the hyperthermophilic archaeum *Pyrococcus horikoshii* OT3. *Extremophiles* 9, 127–134.
- Pappenberger, G., Wilsher, J.A., Roe, S.M., Counsell, D.J., Willison, K.R., and Pearl, L.H. (2002). Crystal structure of the CCT γ apical domain: implications for substrate binding to the eukaryotic cytosolic chaperonin. *J. Mol. Biol.* 318, 1367–1379.
- Rommelaere, H., De Neve, M., Neirynck, K., Peelaers, D., Waterschoot, D., Goethals, M., Fraeyman, N., Vandekerckhove, J., and Ampe, C. (2001). Prefoldin recognition motifs in the nonhomologous proteins of the actin and tubulin families. *J. Biol. Chem.* 276, 41023–41028.
- Scheres, S.H.W., Valle, M., Núñez, R., Sorzano, C.O.S., Marabini, R., Herman, G.T., and Carazo, J.M. (2005). Maximum-likelihood multi-reference refinement for electron microscopy images. *J. Mol. Biol.* 348, 139–149.
- Schüler, H., Lindberg, U., Schutt, C.E., and Karlsson, R. (2000). Thermal unfolding of G-actin monitored with the DNase I-inhibition assay. *Eur. J. Biochem.* 267, 476–486.
- Schwede, T., Kopp, J., Guex, N., and Peitsch, M.C. (2003). SWISS-MODEL: an automated protein homology-modeling server. *Nucleic Acids Res.* 31, 3381–3385.
- Siegers, K., Waldmann, T., Leroux, M.R., Grein, K., Shevchenko, A., Schiebel, E., and Hartl, F.U. (1999). Compartmentation of protein folding in vivo: sequestration of non-native polypeptide by the chaperonin-GimC system. *EMBO J.* 18, 75–84.
- Siegers, K., Böltner, B., Schwarz, J.P., Böttcher, U.M.K., Guha, S., and Hartl, F.U. (2003). TRiC/CCT cooperates with different upstream chaperones in the folding of distinct protein classes. *EMBO J.* 22, 5230–5240.
- Siegert, R., Leroux, M.R., Scheufler, C., Hartl, F.U., and Moarefi, I. (2000). Structure of the molecular chaperone prefoldin: unique interaction of multiple coiled coil tentacles with unfolded proteins. *Cell* 103, 621–632.
- Torrey-Simons, C., Staes, A., Rommelaere, H., Ampe, C., Lewis, S.A., and Cowan, N.J. (2004). Selective contribution of eukaryotic prefoldin subunits to actin and tubulin binding. *J. Biol. Chem.* 279, 4196–4203.
- Vainberg, I.E., Lewis, S.A., Rommelaere, H., Ampe, C., Vandekerckhove, J., Klein, H.L., and Cowan, N.J. (1998). Prefoldin, a chaperone that delivers unfolded proteins to cytosolic chaperonin. *Cell* 93, 863–873.
- Valpuesta, J.M., Carrascosa, J.L., and Willison, K.R. (2005). Structure and function of the cytosolic chaperonin CCT. In *Protein Folding Handbook*, J. Buchner and T. Kiefhaber, eds. (Weinheim, Germany: Wiley-VCH), pp. 725–755.
- Vriend, G. (1990). WHAT IF: a molecular modelling and drug design program. *J. Mol. Graph.* 8, 52–56.

Wriggers, W., Chacón, P., Kovacs, J., Tama, F., and Birmanns, S. (2004). Topology representing neural networks reconcile biomolecular shape, structure, and dynamics. *Neurocomputing* 56, 365–379.

Yoshida, T., Ideno, A., Hiyamuta, S., Yohda, M., and Maruyama, T. (2001). Natural chaperonin of the hyperthermophilic archaeum, *Ther-*

mococcus strain KS-1: a hetero-oligomeric chaperonin with variable subunit composition. *Mol. Microbiol.* 39, 1406–1413.

Zako, T., Iizuka, R., Okochi, M., Nomura, T., Ueno, T., Tadakuma, H., Yohda, M., and Funatsu, T. (2005). Facilitated release of substrate protein from prefoldin by chaperonin. *FEBS Lett.* 579, 3718–3724.